Nonlinear Least-Square Estimation (LSE)-based Parameter Identification of a Synchronous Generator

Yangkun Xu, *Student Member, IEEE*, Yin Li, *Student Member, IEEE*, Zhixin Miao, *Senior Member, IEEE*

***Abstract*—The objective of this paper is to identify a synchronous generator's internal voltage, dq-axis reactances using Phasor Measurement Unit (PMU) data obtained at the terminal bus of the generator. Our approach is to firstly classify the PMU data into inputs and outputs and then identify the relationship between the inputs and the outputs. With different classifications and different assumptions on salience, we obtain three different estimation models. With the the relationship expressed by nonlinear algebraic equations given, we then apply nonlinear least-square estimation (LSE) and regulated nonlinear LSE to conduct parameter estimation. Case studies are conducted to illustrate the estimation procedure.**

***Index Terms*—Nonlinear least-square estimation, Parameter estimation, Phasor Measurement Unit (PMU), Synchronous generator.**

I. Introduction

Accurate estimation of synchronous generator parameters and state variables plays an important role in predicting the dynamic performance of the power system that is crucial to ensure its stability and reliability [1], [2]. In recent years, Phasor Measurement Unit (PMU) is developed in power systems. Although PMU cannot capture the electromagnetic dynamics properly due to its lower sampling rate (20-100Hz) [3]–[6], the electromechanical dynamics can be reflected. PMU data has become more and more popular on identification and optimization [3], [7]–[9]. If a PMU is installed at the terminal of a synchronous generator, it can provide PMU measurements including the terminal bus voltage, bus voltage phase angle, real power, and reactive power.

Both of the non-salient generator and the salient generator are considered in this paper. Non-salient generator is assumed to be a reactance X_d behind a constant voltage (E_a). These two parameters can be estimated based on three measurements from a PMU at the terminal bus of the generator. The measurement data will be treated as the system's inputs and outputs. For non-salient generator, there are two different ways to classify the data into inputs and outputs. They are named as Model 1 and Model 2 in Section II.

Furthermore, salience of a generator is considered. Model 3 is designed to estimate parameters including the internal voltage E_a, d-axis reactance X_d and the q-axis reactance X_q with the same three PMU measurements.

As one of major estimation methods, nonlinear LSE is used as the main tool in this paper. First, the input/output nonlinear relationships are formulated by algebraic equations corresponding to different estimation models. Then, nonlinear LSE is solved using Gauss-Newton method to estimate the unknown parameters of a synchronous generator.

Y. Xu, Y. Li, and Z. Miao are with Dept. of Electrical Engineering, University of South Florida, Tampa FL 33620. Email: zmiao@usf.edu

The remainder of this paper is organized as follows. Section II introduces three estimation models in three sub-sections respectively. The topology of the system is also mentioned in Section II. Section III shows the case studies. The measurement data are obtained from time-domain simulations built in MATLAB/Simulink. With the measurement data, parameter estimation is carried out and the estimated values are compared with the real values used for time-domain simulations. Section VI concludes the paper. The parameters used in the time-domain simulation are listed in Appendix.

II. Estimation Models

There are three estimation models are proposed in this paper. All of them are based on the synchronous machine model shown in Fig. 1. The synchronous generator model includes the swing dynamics, rotor flux dynamics, automatic voltage regulator (AVR), and turbine-governor (TG). PMU is normally installed at the terminal bus of the generator. We can obtain the measurements of the terminal bus voltage V_a, terminal bus angle θ_a, real power P_e, and reactive power Q_e of the generator by using PMU measurements.

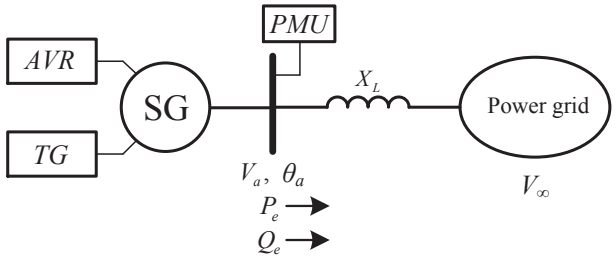

Fig. 1: Synchronous generator connected to infinite bus through a transmission line.

A. Model 1: PV as inputs and Q as output

In the first two estimation models, the salience of synchronous generator is not considered so the d-axis reactance is equal to the q-axis reactance (X_d=X_q). In addition, it is assumed that the generator resistance is neglected compared with its reactance. Hence, the real and reactive power of the generator can be expressed by the following equations:

$$\begin{cases} P_e = \frac{E_a V_a}{X_d} \sin(\delta_m) \\ Q_e = \frac{E_a V_a \cos(\delta_m) - V_a^2}{X_d} \end{cases} \tag{1}$$

where δ_m is phase angle difference between the angles of E_a and V_a shown in Fig. 2.

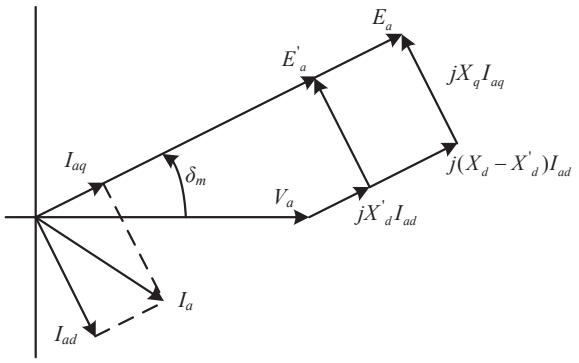

Fig. 2: Phasor diagram shows the relation among E_a, V_a and δ_m.

In Model 1, to avoid estimating rotor angle δ_m, equations (1) can be converted to a equation for Q_e (2) using several steps:

$$\begin{aligned}(E_aV_a)^2 &= (E_aV_a\sin(\delta_m))^2 + (E_aV_a\cos(\delta_m))^2\\ (E_aV_a)^2 &= (P_eX_d)^2 + (Q_eX_d + V_a^2)^2\\ \implies Q_e &= \sqrt{\left(\frac{E_aV_a}{X_d}\right)^2 - P_e^2} - \frac{V_a^2}{X_d}\end{aligned} \tag{2}$$

The difficulty here is that the internal voltage E_a is not possible to be measured. In the case studies, a sudden load change only causes the small variation of E_a. Therefore, it is assumed that the E_a is an internal variable and its final steady-state condition is considered as parameters to be estimated. In Model 1, E_a and X_d are two constant parameters which require to be estimated. We introduce two new parameters, a and b, to replace $(\frac{E_a}{X_d})^2$ and $\frac{1}{X_d}$. Then, (2) is rewritten as (3) which is used to design Model 1.

$$Q_e = \sqrt{aV_a^2 - P_e^2} - bV_a^2 \tag{3}$$

This algebraic equation contains two parameters a and b to be estimated. The input vector is $\boldsymbol{u} = \begin{bmatrix}P_e & V_a\end{bmatrix}^T$ and the output vector is $\boldsymbol{y} = Q_e$.

The nonlinear LSE can be solved iteratively using Gauss-Newton method. The estimated reactive power $\hat{Q}_e$ can be calculated using (3) with the input data $\boldsymbol{u}$, and an assumed $\boldsymbol{x} = \begin{bmatrix}a & b\end{bmatrix}^T$. Let us expand nonlinear equation in Taylor series and stopping at the second term. A linear LSE problem is built up as follows:

$$Q_e(\text{measured}) \approx \hat{Q}_{e_k} + \boldsymbol{F}_k\boldsymbol{d}_k \tag{4}$$

where $\boldsymbol{F}$ matrix is the Jacobian matrix of partial derivatives of (3) with respect to a and b. $\boldsymbol{d}$ vector is the Gauss-Newton correction. k means the iterations step ($k \geq 0$). The above problem can be expressed by (5).

$$\underbrace{\begin{bmatrix}\Delta Q_{e_1}\\ \Delta Q_{e_2}\\ \vdots\\ \Delta Q_{e_n}\end{bmatrix}}_{\boldsymbol{r}} = \underbrace{\begin{bmatrix}\frac{\partial Q_{e_1}}{\partial a} & \frac{\partial Q_{e_1}}{\partial b}\\ \frac{\partial Q_{e_2}}{\partial a} & \frac{\partial Q_{e_2}}{\partial b}\\ \vdots & \vdots\\ \frac{\partial Q_{e_n}}{\partial a} & \frac{\partial Q_{e_n}}{\partial b}\end{bmatrix}}_{\boldsymbol{F}} \cdot \underbrace{\begin{bmatrix}\Delta a\\ \Delta b\end{bmatrix}}_{\boldsymbol{d}} \tag{5}$$

where $\boldsymbol{r}$ vector is the residual vector of the measurement Q_e and its estimation $\hat{Q}_e$. The subscripts, 1 to n, is corresponding to each step of measurements. In this paper, the sampling rate of PMU is 100Hz so n will be 1000 if 10-second measurements are used for estimation.

$\boldsymbol{d}$ can be identified directly using the normal equation of LSE in (6) and updated in each iteration.

$$\boldsymbol{d}_k = (\boldsymbol{F}_k^T\boldsymbol{F}_k)^{-1}\boldsymbol{F}_k^T\boldsymbol{r}_k \tag{6}$$

At the first iteration, $\boldsymbol{x}_0$ was evaluated based on the initial vector, $\boldsymbol{\theta}_0 = \begin{bmatrix}E_a & X_d\end{bmatrix}^T$ for Model 1. The selection range of $\boldsymbol{\theta}_0$ will be discussed in Case Studies. The lengths of both $\boldsymbol{x}$ and $\boldsymbol{\theta}$ are dependent on $\boldsymbol{d}$ so they are different in other two modes. For the next iterations, $\boldsymbol{x}_k$ is updated using (7) to calculate new $\hat{Q}_e$.

$$\underbrace{\begin{bmatrix}a_{k+1}\\ b_{k+1}\end{bmatrix}}_{\boldsymbol{x}_{k+1}} = \underbrace{\begin{bmatrix}a_k\\ b_k\end{bmatrix}}_{\boldsymbol{x}_k} + \underbrace{\begin{bmatrix}\Delta a_k\\ \Delta b_k\end{bmatrix}}_{\boldsymbol{d}_k} \tag{7}$$

After enough iterations, a and b can be estimated successfully. Then, it is easy to calculate E_a and X_d based on estimated $\boldsymbol{x}$.

$Remark$: Although LSE method in (6) is able to estimate $\boldsymbol{d}$, it cannot guaranteed that the precise solution in the strict sense. In another word, the proposed estimation approach will fail to produce the accurate estimation if matrix inversion, $\boldsymbol{F}_k^T\boldsymbol{F}_k$, has the singularity issue.

To overcome the aforementioned issue, we need to improve (6) by adding $\lambda\boldsymbol{I}$ in the inverse matrix [10]. This formula first derived by Tikhonov in 1963 [11].

$$\boldsymbol{d}_k = (\boldsymbol{F}_k^T\boldsymbol{F}_k + \lambda\boldsymbol{I})^{-1}\boldsymbol{F}_k^T\boldsymbol{r}_k \tag{8}$$

where $\boldsymbol{I}$ is the identity matrix and λ is called the regularization parameter which is greater than zero. The effect of this λ will be indicated in Case Studies.

B. Model 2: V_a as input and PQ as outputs

Compared with Model 1, Model 2 has one input signal V_a and two output signals P_e and Q_e. Also, it can be used to estimate the dynamic parameter, rotor angle δ_m, since Model 2 considers δ_m in the power equation (9) as follows:

$$\begin{cases}P_e = aV_a\sin(\delta_m)\\ Q_e = aV_a\cos(\delta_m) - bV_a^2\end{cases} \tag{9}$$

where $a = \frac{E_a}{X_d}$ and $b = \frac{1}{X_d}$.

Considering Model 2 use the same estimation methodology, the linear LSE model is built as follows:

$$\begin{bmatrix} \Delta P_{e_1} \\ \Delta P_{e_2} \\ \vdots \\ \Delta P_{e_n} \\ \Delta Q_{e_1} \\ \Delta Q_{e_2} \\ \vdots \\ \Delta Q_{e_n} \end{bmatrix} = \left[\begin{array}{cccc|cc} \frac{\partial P_{e_1}}{\partial \delta_{m_1}} & 0 & \cdots & 0 & \frac{\partial P_{e_1}}{\partial a} & \frac{\partial P_{e_1}}{\partial b} \\ 0 & \frac{\partial P_{e_2}}{\partial \delta_{m_2}} & \cdots & 0 & \frac{\partial P_{e_2}}{\partial a} & \frac{\partial P_{e_2}}{\partial b} \\ \vdots & \vdots & \ddots & \vdots & \vdots & \vdots \\ 0 & 0 & \cdots & \frac{\partial P_{e_n}}{\partial \delta_{m_n}} & \frac{\partial P_{e_n}}{\partial a} & \frac{\partial P_{e_n}}{\partial b} \\ \hline \frac{\partial Q_{e_1}}{\partial \delta_{m_1}} & 0 & \cdots & 0 & \frac{\partial Q_{e_1}}{\partial a} & \frac{\partial Q_{e_1}}{\partial b} \\ 0 & \frac{\partial Q_{e_2}}{\partial \delta_{m_2}} & \cdots & 0 & \frac{\partial Q_{e_2}}{\partial a} & \frac{\partial Q_{e_2}}{\partial b} \\ \vdots & \vdots & \ddots & \vdots & \vdots & \vdots \\ 0 & 0 & \cdots & \frac{\partial Q_{e_n}}{\partial \delta_{m_n}} & \frac{\partial Q_{e_n}}{\partial a} & \frac{\partial Q_{e_n}}{\partial b} \end{array}\right] \cdot \begin{bmatrix} \Delta\delta_{m_1} \\ \Delta\delta_{m_2} \\ \vdots \\ \Delta\delta_{m_n} \\ \Delta a \\ \Delta b \end{bmatrix} \tag{10}$$

Compared to Model 1, the length of $\boldsymbol{r}$ in Model 2 is doubled since it consists of two output measurements, ΔP_e and ΔQ_e. The length of $\boldsymbol{d}$ increases to $n+2$ because the number of estimated δ_m is dependent on how many steps of measurements used for the estimation.

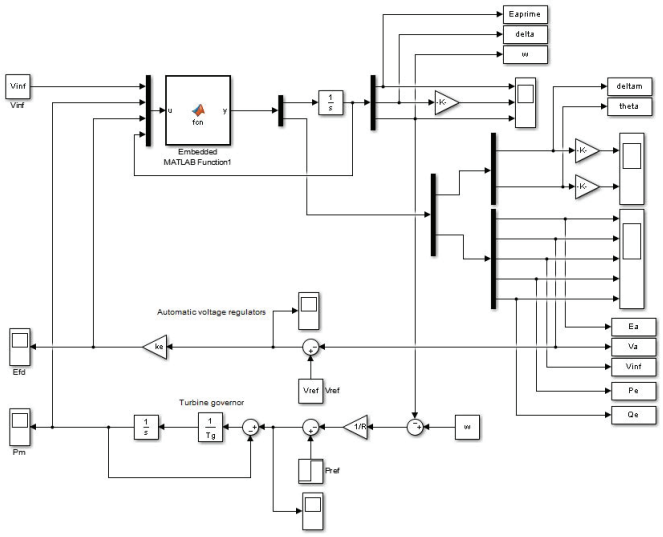

Fig. 3: Matlab/Simulink simulation model.

C. Model 3: V_a as input and PQ as outputs considering salience

Model 3 has the same input and outputs as with Model 2 but it considers a salient pole ($X_d \neq X_q$). With the salience, the power equations, (11), become more complex:

$$\begin{cases} P_e = \frac{E_a V_a}{X_d}\sin(\delta_m) + \frac{V_a^2}{2}\left(\frac{1}{X_q} - \frac{1}{X_d}\right)\sin(2\delta_m) \\ Q_e = \frac{E_a V_a}{X_d}\cos(\delta_m) - V_a^2\left(\frac{\cos^2(\delta_m)}{X_d} + \frac{\sin^2(\delta_m)}{X_q}\right) \end{cases} \tag{11}$$

Re-express (11) using three new parameters a, b, and c:

$$\begin{cases} P_e = aV_a\sin(\delta_m) + \frac{V_a^2}{2}(c-b)\sin(2\delta_m) \\ Q_e = aV_a\cos(\delta_m) - V_a^2\left(b\cos^2(\delta_m) + c\sin^2(\delta_m)\right) \end{cases} \tag{12}$$

where $a = \frac{E_a}{X_d}$, $b = \frac{1}{X_d}$, and $c = \frac{1}{X_q}$. In (12), besides dynamic state δ_m, there are three unknown parameters. Hence, $\boldsymbol{d}$ include $\Delta\delta_m$, Δa , Δb and Δc. Model 3 is expressed by the new $\boldsymbol{d}$ and $\boldsymbol{F}$ as:

$$\begin{bmatrix} \Delta P_{e_1} \\ \Delta P_{e_2} \\ \vdots \\ \Delta P_{e_n} \\ \Delta Q_{e_1} \\ \Delta Q_{e_2} \\ \vdots \\ \Delta Q_{e_n} \end{bmatrix} = \left[\begin{array}{cccc|ccc} \frac{\partial P_{e_1}}{\partial \delta_{m_1}} & 0 & \cdots & 0 & \frac{\partial P_{e_1}}{\partial a} & \frac{\partial P_{e_1}}{\partial b} & \frac{\partial P_{e_1}}{\partial c} \\ 0 & \frac{\partial P_{e_2}}{\partial \delta_{m_2}} & \cdots & 0 & \frac{\partial P_{e_2}}{\partial a} & \frac{\partial P_{e_2}}{\partial b} & \frac{\partial P_{e_2}}{\partial c} \\ \vdots & \vdots & \ddots & \vdots & \vdots & \vdots & \vdots \\ 0 & 0 & \cdots & \frac{\partial P_{e_n}}{\partial \delta_{m_n}} & \frac{\partial P_{e_n}}{\partial a} & \frac{\partial P_{e_n}}{\partial b} & \frac{\partial P_{e_n}}{\partial c} \\ \hline \frac{\partial Q_{e_1}}{\partial \delta_{m_1}} & 0 & \cdots & 0 & \frac{\partial Q_{e_1}}{\partial a} & \frac{\partial Q_{e_1}}{\partial b} & \frac{\partial Q_{e_1}}{\partial c} \\ 0 & \frac{\partial Q_{e_2}}{\partial \delta_{m_2}} & \cdots & 0 & \frac{\partial Q_{e_2}}{\partial a} & \frac{\partial Q_{e_2}}{\partial b} & \frac{\partial Q_{e_2}}{\partial c} \\ \vdots & \vdots & \ddots & \vdots & \vdots & \vdots & \vdots \\ 0 & 0 & \cdots & \frac{\partial Q_{e_n}}{\partial \delta_{m_n}} & \frac{\partial Q_{e_n}}{\partial a} & \frac{\partial Q_{e_n}}{\partial b} & \frac{\partial Q_{e_n}}{\partial c} \end{array}\right] \cdot \begin{bmatrix} \Delta\delta_{m_1} \\ \Delta\delta_{m_2} \\ \vdots \\ \Delta\delta_{m_n} \\ \Delta a \\ \Delta b \\ \Delta c \end{bmatrix} \tag{13}$$

In Model 3, E_a and X_d can be estimated, along with X_q.

III. Case studies

To generate the time-domain measurements, a nonlinear model of the synchronous generator connected to infinite bus system was built in MATLAB/SIMULINK. The screenshot of the nonlinear model is shown in Fig. 3. The model building exploits the vector feature of MATLAB. The details of the technology are described in our previous papers [12]–[14].

The values of nonlinear model parameters used for the time-domain simulation as well as in the theoretical calculation are provided in APPENDIX. The duration of the simulation was 50 seconds and the step size was 0.01s. In another word, the sampling rate of the measurement was 100Hz. Considering that a sudden load change event is more likely happen than a three-phase fault, 10% step change was applied to the mechanical power reference P_{ref} at 5 sec. Corresponding to the non-salient generator and the salient generator, there were two groups of measurements. Fig. 4 shows the time-domain simulation results of salient generator model. V_a, P_e and Q_e were treated as input and output measurements that used for estimation while E_a and δ_m were used to verify the corresponding estimated values. The simulation results of non-salient generator model were very similar with results in Fig. 4, so they were not plotted.

For the better accuracy of the estimation, we should avoid the measurements in flat run or large step response. Therefore, the measurements are acquired from 20s to 40s. In another word, the estimation portion is 20 seconds and total sampling number n of the matrix is 2001. For better visualizing the dynamic details of input and output measurements, we zoomed in three measurements, V_a, P_e, and Q_e, in the estimation portion as shown in Fig. 5.

After the time-domain measurements are obtained, the values of parameters can be estimated following many steps. Taking Model 1 as an example, the required steps for the estimation are summarized as follows:

1. Compute $\boldsymbol{x}_0$ based on the selection of initial vector $\boldsymbol{\theta}_0$
2. Injection of the collected measurements into model 2 in (5)
3. Execution of Nonlinear LSE with GN method. For $k = 0$,
   1) Produce Jacobian matrix $\boldsymbol{F}_k$ using $\boldsymbol{x}_k$
   2) Compute the first set of estimated $\hat{Q}_{e\_k}$ using $\boldsymbol{x}_k$
   3) Compute $\boldsymbol{r}_k$ using $\hat{Q}_{e\_k}$ and measurement Q_{e_k}
   4) Compute $\hat{\boldsymbol{d}}_k$ utilizing LSE method and check the condi-

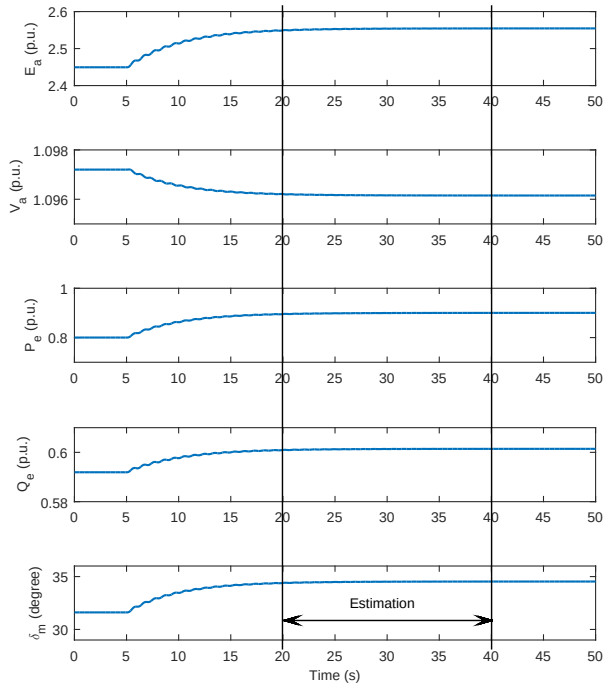

Fig. 4: The time-domain simulation results plotted in the following order: stator open circuit voltage E_a, terminal voltage V_a, electrical active power P_e, reactive power Q_e and rotor angle δ_m.

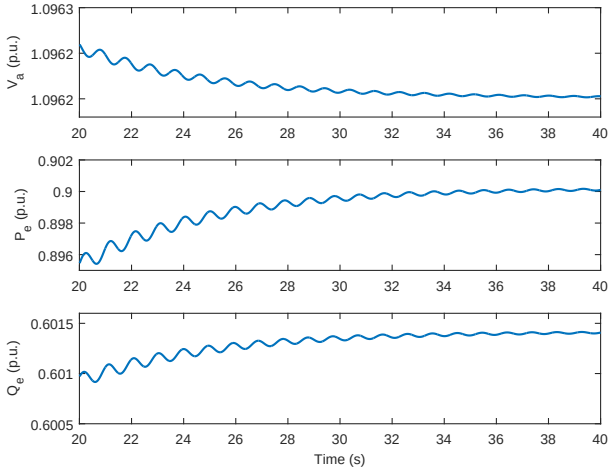

Fig. 5: Three measurements were used for the estimation.

tion number of matrix $\boldsymbol{F}_k^T \boldsymbol{F}_k$

5) Update $\boldsymbol{x}_k$

end

4. Repeat Step 3 until $\hat{\boldsymbol{d}}$ is approaching zero and achieve convergence

5. Compute $\boldsymbol{\theta}_{\text{estimated}}$ based on the values of $\boldsymbol{x}_k$ at the final iteration.

Gauss-Newton method is largely dependent on the selection of the initial vector, $\boldsymbol{\theta}_0$. Thus there should be an acceptable range of the initial vector [2]. In another word, the range which these estimation models can be applied to is limited. Therefore, we did not only test the estimation accuracies of three models, but also determined the acceptable ranges of the initial values of E_a, X_d, X_q, and the first rotor angle, δ_{m1}. The difference between the initial value and the actual value is noted as $\text{error}_{\text{ini}}$.

$$\text{error}_{\text{ini}} = \left| \frac{\boldsymbol{\theta}_0 - \boldsymbol{\theta}_{\text{actual}}}{\boldsymbol{\theta}_{\text{actual}}} \right| \times 100\% \tag{14}$$

where $\boldsymbol{\theta}_{\text{actual}}$ is actual values of state variables and parameters. The errors between the estimated values and actual values, $\text{error}_{\text{est}}$, are used to judge the accuracy. It can be obtained as follows:

$$\text{error}_{\text{est}} = \frac{\boldsymbol{\theta}_{\text{estimated}} - \boldsymbol{\theta}_{\text{actual}}}{\boldsymbol{\theta}_{\text{actual}}} \times 100\% \tag{15}$$

To find the acceptable range of the initial vector, each of estimation model was tested for multiple times with different initial vector. Normally, the estimation method is considered working well if $\text{error}_{\text{est}}$ is below 5% [15], [16]. Hence, the initial vectors which caused one of the errors up closed to 5% were considered as the limits of the range. Both of upper limit and lower limit would be determined.

A. Model 1: Q as input and PV as outputs

Fig. 6 (b) shows that two estimated parameters a and b in Model 1 converged after two iterations with the regulation; then, using the estimated values of a and b, $\boldsymbol{\theta}_{est}$ could be calculated to compare with $\boldsymbol{\theta}_{actual}$. After testing many initial vectors, the limits of the initial vector $\boldsymbol{\theta}_0$ of Model 1 were found as -25% and 60% of the actual values. Table I contains the initial values, estimated values, actual values, and errors which were under the margin conditions.

$Remark$: The effect of regulation was indicated by the converging process of the estimated parameters shown in Fig. 6. In Fig. 6(a), the convergence was almost stopped after seven iterations but the errors of E_a and X_d were 55% and 93%. It indicated that the estimation was not accurate at all without the regulation. With the regulation $\lambda = 1$, the errors of E_a and X_d were under 5% based on the estimated values of a and b shown in Fig. 6(b).

B. Model 2: V as input and PQ as outputs

Based on the estimation results, the rotor angle δ_{m1} was sensitive since its initial value could not exceed -1.5% and $+2\%$ of the actual value. However, the ranges of the internal voltage E_a and d-axis reactance X_d were from -20% to $+30\%$. All of results are tabulated in Table II. Because δ_{m1} is too sensitive, the limits in Table II and Table III presented E_a, X_d and E_a, X_d, X_q, respectively. Fig. 7 (b) verified that the estimated parameters converged at the second iteration.

Different than E_a, X_d, and X_q, the rotor angle δ_m is a dynamic state, so the estimated rotor angle and the actual rotor angle were plotted in time domain shown in Fig. 8.

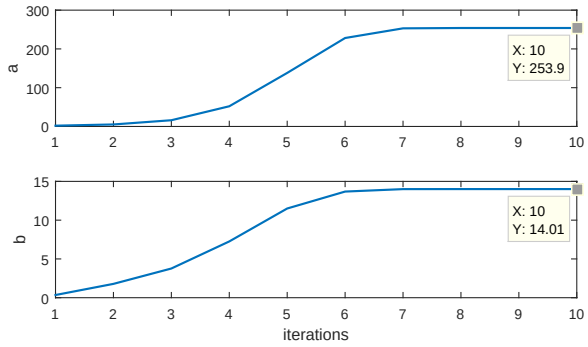

(a) Without regularization

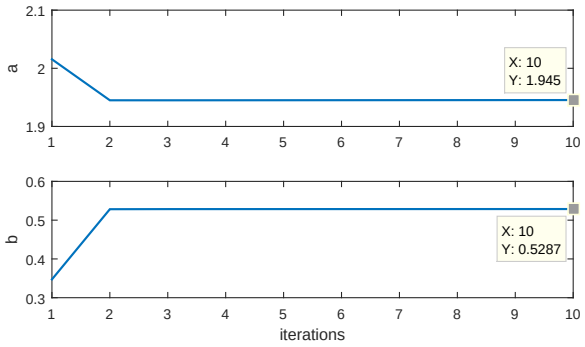

(b) With regularization.

Fig. 6: Model 1: converging process of the estimated parameters.

TABLE I: Identification results of Model 1 of a synchronous generator

Parameters	Actual	$\text{error}_{\text{ini}}$ = -25%			$\text{error}_{\text{ini}}$ =60%		
		Initial	Estimation	$\text{error}_{\text{est}}(\%)$	Initial	Estimation	$\text{error}_{\text{est}}(\%)$
E_a	2.5554	1.9166	2.4787	3 %	4.0887	2.6382	3.24%
X_d	1.8	1.35	1.7175	4.6%	2.88	1.8915	5.086%

TABLE II: Identification results of Model 2 of a synchronous generator

Parameters	Actual	$\text{error}_{\text{ini}}$ =-20%			$\text{error}_{\text{ini}}$ =30%		
		Initial	Estimation	$\text{error}_{\text{est}}(\%)$	Initial	Estimation	$\text{error}_{\text{est}}(\%)$
δ_{m_1}	0.6006	0.5917	0.5931	1.2%	0.6127	0.6109	1.7%
E_a	2.5554	2.0443	2.4818	2.9%	3.322	2.6259	2.8%
X_d	1.8	1.44	1.721	4.4%	2.34	1.8781	4.3%

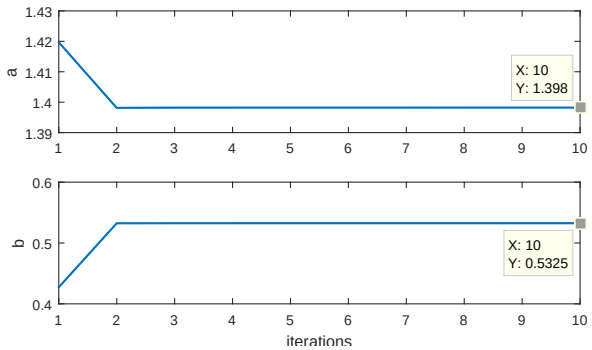

Fig. 7: Model 2: converging process of the estimated parameters.

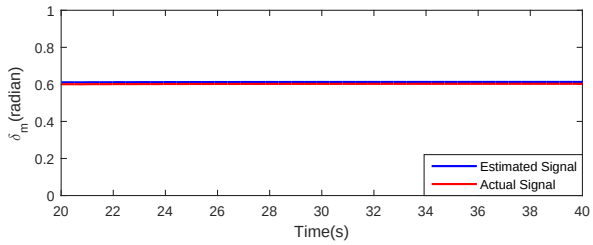

Fig. 8: Model 2: Actual and estimated signals for the rotor angle with respect to the machine terminal.

The discrepancy between the estimated value and actual value was very small ($< 2\%$). Therefore, we considered that the matching degree was adequately high to show the validity of the estimation of rotor angle.

C. Model 3: V as input and PQ as outputs considering saliency

Three converged parameters shown in Fig. 9 verified Model 3 work well. The rotor angle in Model 3 was sensitive, too. The range was between -1.5% and 2%. For rest of parameters, E_a, X_d and X_q, the lower and upper limits was -5% and $+10\%$. Every value was concluded in Table III.

Fig. 10 shows that Model 3 had small difference between the estimated rotor angle and the actual rotor angle.

IV. Conclusion

This paper investigates the nonlinear least square estimation with Gauss-Newton in three different estimation models for synchronous generator identification. Only three measurements are used to do estimation and they are treated as inputs or outputs in different estimation models respectively. To obtain the time-domain simulation results, a nonlinear synchronous generator model was built in MATLAB/Simulink. According to the results, all of three estimation models can be demonstrated to estimate generator parameters accurately. Moreover, what ranges of initial values these models can be applied for are determined. The nonlinear generator model includes electromechanical dynamics, turbine-governor dynamics and excitation dynamics. Therefore, it is considered that these estimation models can be applied to PMU data.

TABLE III: Identification results of Model 3 of a synchronous generator

Parameters	Actual	$\text{error}_{\text{ini}}$ =-5%			$\text{error}_{\text{ini}}$ =10%		
		Initial	Estimation	$\text{error}_{\text{est}}(\%)$	Initial	Estimation	$\text{error}_{\text{est}}(\%)$
δ_{m_1}	0.6004	0.588	0.5893	1.85	0.612	0.6103	1.65%
E_a	2.5546	2.2991	2.45	4.1	2.81	2.6398	3.3%
X_d	1.8	1.62	1.6875	6.2	1.98	1.8938	5.2%
X_q	1.7	1.53	1.6078	5.4	1.87	1.7685	4.03%

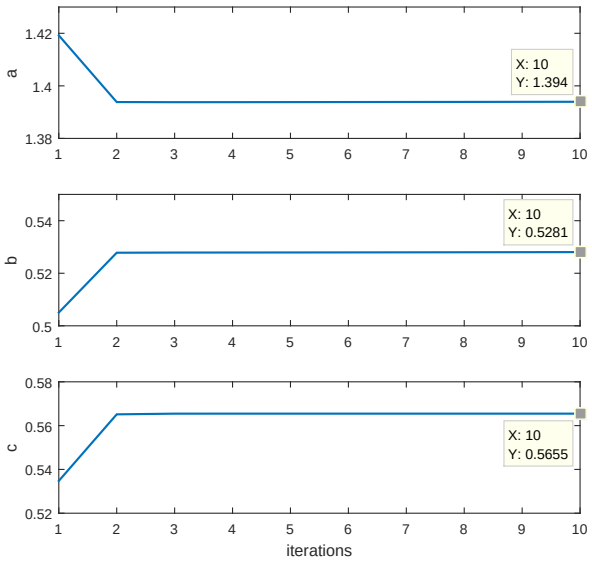

Fig. 9: Model 3: converging process of the estimated parameters.

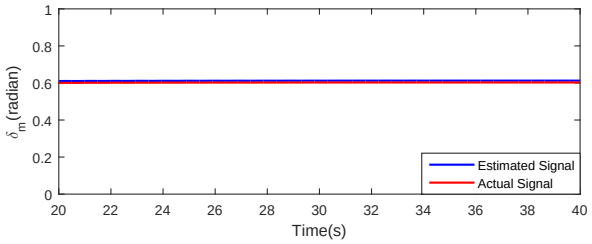

Fig. 10: Model 3: Actual and estimated signals for the rotor angle with respect to the machine terminal.

APPENDIX

Generator model data is listed as follows:

$$H = 6.5s \quad T'_{do} = 2s \quad D = 0.1 \quad X_d = 1.8 \quad X'_d = 0.3$$
$$X_q = 1.7 \quad X_{line} = 0.2 \quad T_g = 1s \quad R = 0.04 \quad k_e = 100$$

All quantities, except time constants, are in per unit.

REFERENCES

[1] F. C. Schweppe, "Power system static-state estimation, part iii: Implementation," *IEEE Transactions on Power Apparatus and Systems*, vol. PAS-89, no. 1, pp. 130–135, Jan 1970.

[2] P. Kundur, N. J. Balu, and M. G. Lauby, *Power system stability and control*. McGraw-hill New York, 1994, vol. 7.

[3] S. Toscani, C. Muscas, and P. A. Pegoraro, "Design and performance prediction of space vector-based pmu algorithms," *IEEE Transactions on Instrumentation and Measurement*, vol. 66, no. 3, pp. 394–404, March 2017.

[4] A. T. Mathew and M. N. Aravind, "Pmu based disturbance analysis and fault localization of a large grid using wavelets and list processing," in *2016 IEEE Region 10 Conference (TENCON)*, Nov 2016, pp. 879–883.

[5] P. H. Gadde, M. Biswal, S. Brahma, and H. Cao, "Efficient compression of pmu data in wams," *IEEE Transactions on Smart Grid*, vol. 7, no. 5, pp. 2406–2413, Sept 2016.

[6] T. A. Bhatti, A. Raheem, T. Alam, M. O. Malik, and A. Munir, "Implementation of low cost non-dft based phasor measurement unit for 50 hz power system," in *2016 International Conference on Computing, Electronic and Electrical Engineering (ICE Cube)*, April 2016, pp. 120–125.

[7] K. G. Khajeh, E. Bashar, A. M. Rad, and G. B. Gharehpetian, "Integrated model considering effects of zero injection buses and conventional measurements on optimal pmu placement," *IEEE Transactions on Smart Grid*, vol. 8, no. 2, pp. 1006–1013, March 2017.

[8] S. Brahma, R. Kavasseri, H. Cao, N. R. Chaudhuri, T. Alexopoulos, and Y. Cui, "Real-time identification of dynamic events in power systems using pmu data, and potential applications 8212;models, promises, and challenges," *IEEE Transactions on Power Delivery*, vol. 32, no. 1, pp. 294–301, Feb 2017.

[9] E. R. Fernandes, S. G. Ghiocel, J. H. Chow, D. E. Ilse, D. D. Tran, Q. Zhang, D. B. Bertagnolli, X. Luo, G. Stefopoulos, B. Fardanesh, and R. Robertson, "Application of a phasor-only state estimator to a large power system using real pmu data," *IEEE Transactions on Power Systems*, vol. 32, no. 1, pp. 411–420, Jan 2017.

[10] A. Neumaier, "Solving ill-conditioned and singular linear systems: A tutorial on regularization," *SIAM review*, vol. 40, no. 3, pp. 636–666, 1998.

[11] A. N. Tihonov, "Solution of incorrectly formulated problems and the regularization method," *Soviet Math*, vol. 4, pp. 1035–1038, 1963.

[12] Z. Miao and L. Fan, "The art of modeling and simulation of induction generator in wind generation applications using high-order model," *Simulation Modelling Practice and Theory*, vol. 16, no. 9, pp. 1239–1253, 2008.

[13] L. Fan, R. Kavasseri, Z. L. Miao, and C. Zhu, "Modeling of dfig-based wind farms for ssr analysis," *Power Delivery, IEEE Transactions on*, vol. 25, no. 4, pp. 2073–2082, 2010.

[14] Y. Li and L. Fan, "Determine power transfer limits of an smib system through linear system analysis with nonlinear simulation validation," in *2015 North American Power Symposium (NAPS)*, Oct 2015, pp. 1–6.

[15] T. G. Landgraf, E. P. T. Cari, and L. F. C. Alberto, "Online parameter estimation of synchronous generators from accessible measurements," in *2016 IEEE/PES Transmission and Distribution Conference and Exposition (T D)*, May 2016, pp. 1–5.

[16] J. C. N. Pantoja, A. Olarte, and H. Daz, "Simultaneous estimation of exciter, governor and synchronous generator parameters using phasor measurements," in *2014 Electric Power Quality and Supply Reliability Conference (PQ)*, June 2014, pp. 43–49.